Journal of Statistical Physics, Vol. 41, 1/2, 1985

On Surface Properties of a Weakly-Coupled Classical One-Component Plasma: The Size Effect in Finite Systems

M. Hasegawa[1] **and M. Watabe**[1]

Received January 11, 1985; revision received March 14, 1985

The surface properties of a weakly coupled classical one-component plasma of finite size are calculated exactly within the Poisson–Boltzmann (PB) approximation scheme. It is found that the ion density profile and the surface energy for a spherical system show strong size dependence. The surface energy also strongly depends on the position of the hard wall introduced for achieving an appropriate equilibrium ion configuration. These results indicate that the recent Monte Carlo simulation data for a spherical system must be interpreted, at least in the weak-coupling regime, as including substantial size effects and cannot be directly compared with the theoretical calculations for the planar surface. For a slab, on the other hand, such size effects are found to be very small if the hard wall is placed at sufficiently distant position from the surface. The dominant contribution to the surface energy which is omitted in the PB approximation is also estimated by the perturbation calculations.

KEY WORDS: Classical one-component plasma; surface properties; density-gradient expansion; Poisson–Boltzmann approximation; Monte Carlo simulations.

1. INTRODUCTION

The classical one-component plasma (OCP) is a system of point-like charged particles (which we call ions) in a rigid neutralizing charge background. It is the simplest model of Coulomb systems but provides a useful starting point for understanding real systems such as liquid metals and molten salts. The bulk properties of the OCP are now well established for a wide range of the coupling parameter by a number of theoretical and

[1] Faculty of Integrated Arts and Sciences, Hiroshima University, Hiroshima 730, Japan.

0022-4715/85/1000-0281$04.50/0

numerical simulation studies.[1] Recently, the surface properties of the OCP have also received increasing theoretical attention[2–6] and Monte Carlo (MC) simulation data are now available.[7,8] There also have been some attempts to use the OCP as a reference system in the theory of surface properties of liquid metals.[9–11]

In this paper we are concerned with the surface properties of a weakly coupled OCP. The density functional formalism provides a useful means of studying inhomogeneous systems[12,13] and the density-gradient expansion, one of approximation schemes in this formalism, has been developed for the OCP.[5,9,14] Recently, Rosinberg *et al.*[15] have argued that the square-gradient approximation is inadequate for calculating the surface properties of the OCP even at $\bar{\Gamma}=1$, where $\bar{\Gamma}$ is the bulk plasma parameter. Their argument is based on the serious discrepancy which has been found between their variational calculations and the MC results for the surface energy. We have examined this problem raised by Rosinberg *et al.* and found that two points are overlooked in their argument.[16] The first point is that the coefficient of the square-gradient term used by them in their calculations is not good. In fact, we have shown that part of the discrepancy can be removed for a system of large $\bar{\Gamma}$, in which the gradient term plays an important role, by incorporating an improved coefficient. The second point is that the influence of the finite size on the surface properties could be substantial in the MC simulation for a spherical system. Our variational calculations for a spherical system have actually predicted strong size dependence of the surface properties at $\bar{\Gamma}=1$.[16] Ballone *et al.*[17] have also discussed the influence of the finite size on the interfacial density profile in the presence of an impenetrable wall.

The purpose of this paper is to reexamine such a size effect more rigorously without relying on the variational method. For this purpose we employ the Poisson–Boltzmann (PB) approximation scheme which should be valid in the weak-coupling limit and may be adequate for calculating surface properties of the OCP of small $\bar{\Gamma}$. This approximation scheme has already been applied to the planar surface[15] and the present work is its generalization to a finite system. Recently, Alastuey[18] has also used the PB approximation together with other higher-order theories for calculating the interfacial density profile of the two-dimensional OCP. He has found that even this crudest approximation produces reasonable results for systems with soft wall, the free surface being a typical example. However, it should be noted that the PB approximation is too crude to be used for quantitative purposes in the strong-coupling regime ($\bar{\Gamma}>1$).

We consider two types of finite systems: One is a spherical system, for which MC simulations have been performed,[7,8] and the other is a slab with infinite extent in two dimensions. In the next section we derive simple

expressions for the surface free energy and surface energy of these systems within the PB approximation scheme. These expressions are ready for direct comparisons with those obtained for the planar surface.[15] The results of calculations for the surface density profile and surface energy are presented and compared with the MC simulation results in Section 3. In this section the contribution to the surface energy which is omitted in the PB approximation is also estimated within the local approximation (i.e., improved PB approximation). Concluding remarks are given in the final section.

2. SURFACE PROPERTIES IN THE POISSON–BOLTZMANN APPROXIMATION

We consider a system of ions with charge Ze embedded in a non-uniform neutralizing charge background of density $-en(\mathbf{r})$. The relevant quantity in the density functional formalism is the thermodynamic potential.[12,13] It is the unique functional of the ion density $\rho(\mathbf{r})$ and may be written as

$$\Omega[\rho] = G[\rho] + \frac{e}{2}\int d\mathbf{r}\,[Z\rho(\mathbf{r}) - n(\mathbf{r})]\,\phi(\mathbf{r}) - \mu\int d\mathbf{r}\,\rho(\mathbf{r}) \tag{1}$$

where $G[\rho]$ is the non-Coulombic part of the free energy functional, $\phi(\mathbf{r})$ is the electrostatic potential

$$\phi(\mathbf{r}) = e\int d\mathbf{r}'\,\frac{Z\rho(\mathbf{r}') - n(\mathbf{r}')}{|\mathbf{r} - \mathbf{r}'|} \tag{2}$$

and μ is the chemical potential. The equilibrium ion density may be determined by the stationary condition of $\Omega[\rho]$, or the Euler–Lagrange equation

$$\frac{\delta\Omega[\rho]}{\delta\rho(\mathbf{r})} = \frac{\delta G[\rho]}{\delta\rho(\mathbf{r})} + Ze\phi(\mathbf{r}) - \mu = 0 \tag{3}$$

Here we consider the PB approximation scheme studied by Rosinberg *et al.*[15] for the planar surface. This approximation consists of taking $G[\rho]$ to be the one which is valid for a noninteracting system,[13] i.e.,

$$G[\rho] = \int d\mathbf{r}\; g_0(\rho(\mathbf{r})) \tag{4}$$

where

$$g_0(\rho) = \rho k_B T[\ln \rho - 1 - \ln(Mk_B T/2\pi\hbar^2)^{3/2}] \tag{5}$$

k_B and M being the Boltzmann constant and the ion mass, respectively. Equation (4) is nothing but the local approximation and may be adequate for surface calculations at small $\bar{\Gamma}$ where the gradient term is not important.[5,15,16] $g_0(\rho)$ in Eq. (5) is the free energy density of a homogeneous noninteracting gas of density ρ and it can be viewed as the crucial approximation. In this approximation scheme the Euler–Lagrange equation can be written

$$\mu = \mu_0(\rho(\mathbf{r})) + Ze\phi(\mathbf{r}) \tag{6}$$

where μ_0 is the intrinsic chemical potential given by

$$\mu_0(\rho) = \frac{dg_0(\rho)}{d\rho} = k_B T\left[\ln \rho - \ln\left(\frac{Mk_B T}{2\pi\hbar^2}\right)^{3/2}\right] \tag{7}$$

No further approximation is made and the surface ion density profile and the surface energy are calculated exactly within a numerical accuracy. However, it should be noted that, strictly speaking, the formulation in the above is valid only in the thermodynamic limit and any fluctuation associated with the finiteness of a system will not be taken into account. In the following two sections we consider two situations in which size effects could be appreciable.

2.1. Spherical System

Consider a system of ions confined to a spherical volume of radius R_1. The compensating charge background density is uniform in a spherical volume of radius R_0 ($R_0 < R_1$), i.e.,

$$n(r) = \begin{cases} \bar{n} & (r < R_0) \\ 0 & (r > R_0) \end{cases} \tag{8}$$

The need for introducing a hard wall in a finite system has been discussed by Badiali *et al.*[7]: For a system consisting of a finite number of particles, the most probable configuration of the system would be the one in which all particles are separated from one another by an infinite distance.

For a spherically symmetric system we immediately obtain from (6)

$$\rho(r) = \rho(0)\exp[-Ze\phi(r)/k_B T] \tag{9}$$

where the origin of $\phi(r)$ is chosen such that $\phi(0)=0$. Similarly, the Poisson equation may be written

$$\frac{d}{dr}\left[r^2\frac{d\phi(r)}{dr}\right]=-4\pi e r^2[Z\rho(r)-n(r)] \tag{10}$$

From (9) and (10) we obtain the following differential equation for $\rho(r)$:

$$\begin{aligned}\frac{d}{dr}\left[r^2\frac{\rho'(r)}{\rho(r)}\right]&=-\frac{Ze}{k_BT}\frac{d}{dr}\left[r^2\frac{d\phi(r)}{dr}\right]\\&=\frac{4\pi Ze^2}{k_BT}r^2[Z\rho(r)-n(r)]\end{aligned} \tag{11}$$

Equation (11) is the Poisson–Boltzmann equation generalized to a spherical system. In terms of the reduced variable $u=\kappa r$, where $\kappa^2=4\pi\bar{\rho}(Ze)^2/k_BT$, Eq. (11) is written

$$\frac{d}{du}\left[u^2\frac{\tilde{\rho}'(u)}{\tilde{\rho}(u)}\right]=u^2[\tilde{\rho}(u)-\theta(u_0-u)] \tag{12}$$

where $\tilde{\rho}(u)=\rho(u)/\bar{\rho}$, $Z\bar{\rho}=\bar{n}$ and $u_0=\kappa R_0$. This equation cannot be solved analytically and the numerical method we use will be described in the next section.

Next we consider the excess free energy per unit surface area (which we simply call surface free energy) defined ny

$$\begin{aligned}\gamma&=\frac{1}{4\pi R_0^2}\left\{\int d\mathbf{r}\,[g_0(\rho(r))-g_0(\bar{\rho})\,\theta(R_0-r)]\right.\\&\quad\left.+\frac{e}{2}\int d\mathbf{r}\,[Z\rho(r)-n(r)]\,\phi(r)\right\}\\&=\gamma_0+\gamma_{es}\end{aligned} \tag{13}$$

For a system which satisfies the overall charge neutrality condition, we may set $g_0(\rho)=\rho k_BT\ln\rho$ in Eq. (13). Then we have

$$\begin{aligned}\gamma_0&=k_BTR_0^{-2}\int_0^{R_1}dr\,r^2[\rho(r)\ln\rho(r)-\bar{\rho}\ln\bar{\rho}\theta(R_0-r)]\\&=k_BTR_0^{-2}\int_0^{R_1}dr\,r^2\rho(r)\ln[\rho(r)/\bar{\rho}]\\&=\bar{\rho}k_BTR_0^{-2}\int_0^{R_0}dr\,r^2\ln[\rho(r)/\bar{\rho}]-2\gamma_{es}\end{aligned} \tag{14}$$

where we have used the charge neutrality condition on the second line and Eq. (9) on the third line. The electrostatic term γ_{es} can be calculated as in the following by using the Poisson equation and by integrating by part:

$$\begin{aligned}\gamma_{es} &= -\frac{1}{4\pi}\frac{1}{2R_0^2}\int_0^{R_1} dr\,\phi(r)\frac{d}{dr}\left[r^2\frac{d\phi(r)}{dr}\right] \\ &= \frac{1}{4\pi}\frac{1}{2R_0^2}\int_0^{R_1} dr\,r^2\left[\frac{d\phi(r)}{dr}\right]^2 \\ &= \frac{1}{4\pi}\left(\frac{k_BT}{Ze}\right)^2\frac{1}{2R_0^2}\int_0^{R_1} dr\,r^2\left[\frac{\rho'(r)}{\rho(r)}\right]^2 \end{aligned} \tag{15}$$

where we have used the boundary condition $\phi'(R_1)=0$, which is a consequence of the charge neutrality condition within a sphere of radius R_1 and can be proved by integrating Eq. (10) from 0 to R_1.

From (14) and (15) we have the following expression for γ written in terms of the reduced quantities:

$$\gamma = \bar{\alpha}\bar{\rho}k_BT\frac{1}{(3\bar{\Gamma})^{1/2}}\left\{\frac{1}{u_0^2}\int_0^{u_0} du\,u^2\ln\tilde{\rho}(u) - \frac{1}{2u_0^2}\int_0^{u_1} du\,u^2\left[\frac{\tilde{\rho}'(u)}{\tilde{\rho}(u)}\right]^2\right\} \tag{16}$$

where $\bar{\Gamma}$ is the plasma parameter defined by $\bar{\Gamma}=(Ze)^2/\bar{\alpha}k_BT$, $\bar{\alpha}=(3/4\pi\bar{\rho})^{1/3}$ and $u_1=\kappa R_1$. From Eq. (12) we can derive the relation (the derivation is given in Appendix A)

$$\begin{aligned}\frac{1}{2u_0^2}\int_0^{u_1} du\,u^2\left[\frac{\tilde{\rho}'(u)}{\tilde{\rho}(u)}\right]^2 &= \frac{3}{u_0^2}\int_0^{u_0} du\,u^2\ln\tilde{\rho}(u) \\ &\quad - u_0[1+\ln\tilde{\rho}(u_0)] + \left(\frac{u_1}{u_0}\right)^2 u_1\tilde{\rho}(u_1)\end{aligned} \tag{17}$$

Using (17) in (16) we have the final expression for γ:

$$\begin{aligned}\gamma = \bar{\alpha}\bar{\rho}k_BT\frac{1}{(3\bar{\Gamma})^{1/2}}\Bigg\{&-\frac{2}{u_0^2}\int_0^{u_0} du\,u^2\ln\tilde{\rho}(u) \\ &+ u_0[1+\ln\tilde{\rho}(u_0)] - \left(\frac{u_1}{u_0}\right)^2 u_1\tilde{\rho}(u_1)\Bigg\}\end{aligned} \tag{18}$$

Note that γ is expressed in terms of the ion density in the region $u \leqslant u_0$ and at the hard wall.

The excess internal energy per unit surface area (which we simply call surface energy) can be calculated as in the following:

$$U_s = \gamma - T\frac{\partial \gamma}{\partial T} = \gamma_{es}$$

$$= \bar{\alpha}\bar{\rho}k_B T \frac{1}{(3\bar{\Gamma})^{1/2}} \frac{1}{2u_0^2} \int_0^{u_1} du\, u^2 \left[\frac{\tilde{\rho}'(u)}{\tilde{\rho}(u)}\right]^2$$

$$= \bar{\alpha}\bar{\rho}k_B T \frac{1}{(3\bar{\Gamma})^{1/2}} \left\{ \frac{3}{u_0^2} \int_0^{u_0} du\, u^2 \ln \tilde{\rho}(u) \right.$$

$$\left. - u_0[1 + \ln \tilde{\rho}(u_0)] + \left(\frac{u_1}{u_0}\right)^2 u_1 \tilde{\rho}(u_1) \right\} \tag{19}$$

At this point it is interesting to compare the present results for γ and U_s with those obtained for a planar surface.[15] In the limit $u_0 \to \infty$ with u_1/u_0 fixed at a finite value, Eq. (18) becomes

$$\gamma = \bar{\alpha}\bar{\rho}k_B T \frac{1}{(3\bar{\Gamma})^{1/2}} \left\{ -2 \int_{-\infty}^{0} du \ln \tilde{\rho}(u) + \lim_{u_0 \to \infty} u_0[1 + \ln \tilde{\rho}(0)] \right\} \tag{20}$$

where the origin of the coordinate is taken at the surface. Note that the asymptotic behavior of $\tilde{\rho}(u)$ at large u is given by $\tilde{\rho}(u) \propto u^{-2}$ and hence $u_1 \tilde{\rho}(u_1) = 0$ in the limit $u_1 \to \infty$. Equation (20) is compared with the result of Rosinberg *et al.*[15]

$$\gamma = \bar{\alpha}\bar{\rho}k_B T \frac{2}{(3\bar{\Gamma})^{1/2}} \int_{-\infty}^{0} du \ln \tilde{\rho}(u) \tag{21}$$

The comparison between (20) and (21) implies

$$\lim_{u_0 \to \infty} u_0[1 + \ln \tilde{\rho}(0)] = 4 \int_{-\infty}^{0} du \ln \tilde{\rho}(u) \tag{22}$$

or

$$\lim_{u_0 \to \infty} \tilde{\rho}(0) = \frac{1}{e}\left(1 + \frac{4A}{u_0} + \cdots\right) \qquad (e = 2.718...) \tag{23}$$

where

$$A = \int_{-\infty}^{0} du \ln \tilde{\rho}(u) = -1.08312 \tag{24}$$

This value of A is compared with -1.08206 obtained by Rosinberg *et al.*[15] by an approximate method. The result of Eq. (24) was obtained by using a numerical solution of Eq. (12) in the limit $u_0 \to \infty$ and found to be very accurate. We have confirmed that our numerical solutions $\tilde{\rho}(u)$ for large u_0 really satisfy the tendency given by Eq. (23).

2.2. System of Slab Geometry

In this section we consider a system in which the background density is uniform in a slab with infinite extent in two dimensions and given by

$$n(z) = \begin{cases} \bar{n} & (|z| < L_0) \\ 0 & (|z| > L_0) \end{cases} \tag{25}$$

For this system there is no need of introducing a hard wall to achieve an equilibrium configuration in which the ion density is finite in the region of the background. As far as we know no numerical simulation for a slab has yet appeared in the literature. In such a simulation it would be practical to introduce a hard wall for avoiding a long-range tail of the ion density $\rho(z)$. Here we also introduce a hard wall at $|z| = L_1$ $(L_1 > L_0)$, which enables us to compare the present results with such a numerical simulation.

For a slab we obtain from (6) and (7)

$$\rho(z) = \rho(0) \exp[-Ze\phi(z)/k_B T] \tag{26}$$

where the origin of $\phi(z)$ is taken at $z = 0$, i.e., $\phi(0) = 0$. The Poisson equation for a slab may be written

$$\frac{d^2\phi(z)}{dz^2} = -4\pi e[Z\rho(z) - n(z)] \tag{27}$$

From (26) and (27) we obtain the Poisson–Boltzmann equation

$$\frac{d}{du}\left[\frac{\tilde{\rho}'(u)}{\tilde{\rho}(u)}\right] = \tilde{\rho}(u) - \theta(u_0 - |u|) \tag{28}$$

where $u = \kappa z$ and $u_0 = \kappa L_0$. Note that the form of Eq. (28) is the same as that for a semi-infinite system with planar surface.[5,15]

We are interested in the solution which satisfies the physically acceptable boundary condition $\tilde{\rho}'(0) = 0$. Such a solution satisfies the condition $\tilde{\rho}'(u_1) = 0$, which is again a consequence of the charge neutrality condition

and can be proved by integrating Eq. (28) from 0 to u_1. Note that for $|u| > u_0$ we have an analytic solution to (28),

$$\tilde{\rho}(u) = \frac{2}{(|u| - u_0 + b_0)^2} \qquad (|u| > u_0) \tag{29}$$

where b_0 is a constant which must be determined by the charge neutrality condition. However, this solution does not satisfy the required boundary condition ($\tilde{\rho}'(u_1) = 0$) except in the limit $L_0 \to \infty$ (with L_1/L_0 fixed at a finite value). This limiting case corresponds to a semi-infinite system with planar surface in the absence of a hard wall, for which $b_0 = (2e)^{1/2}$ ($e = 2.718...$).[5,15]

Next we consider the surface free energy defined by

$$\gamma = \frac{1}{2}\int_{-L_1}^{L_1} dz[g_0(\rho(z)) - g_0(\bar{\rho})\,\theta(L_0 - |z|)] + \frac{e}{4}\int_{-L_1}^{L_1} dz[Z\rho(z) - n(z)]\,\phi(z) \tag{30}$$

Using techniques similar to those in Section 2.1, Eq. (30) can be reduced to

$$\gamma = \bar{\alpha}\bar{\rho}k_B T(3\bar{\Gamma})^{-1/2}\left\{2\int_0^{u_0} du \ln \tilde{\rho}(u) - u_0[1 + \ln \tilde{\rho}(u_0)] + u_1\tilde{\rho}(u_1)\right\} \tag{31}$$

for the ion density which satisfies the boundary conditions $\tilde{\rho}'(0) = 0$ and $\tilde{\rho}'(u_1) = 0$ (which is equivalent to the charge neutrality condition), where $u_1 = \kappa L_1$. Similarly, the expression for the surface energy is obtained as

$$U_s = \bar{\alpha}\bar{\rho}k_B T(3\bar{\Gamma})^{-1/2}\left\{-\int_0^{u_0} du \ln \tilde{\rho}(u) + u_0[1 + \ln \tilde{\rho}(u_0)] - u_1\tilde{\rho}(u_1)\right\} \tag{32}$$

The comparison of Eq. (31) with Eq. (21) for the planar surface implies

$$\lim_{u_0 \to \infty} u_0[1 + \ln \tilde{\rho}(u_0)] = 0 \tag{33}$$

We have confirmed that our numerical solutions $\tilde{\rho}(u)$ for large u_0 really satisfy the tendency given by Eq. (33) (see next section).

3. RESULTS OF CALCULATIONS

We first show the results of calculations for a spherical system. Equation (12) was solved numerically by the Runge–Kutta–Gill method by

starting from the initial values of $\tilde{\rho}(u)$ and $\tilde{\rho}'(u)$ well inside the sphere, where $\tilde{\rho}(u)$ can be well approximated by the asymptotic form given by

$$\tilde{\rho}(u) = 1 - b \exp[\beta(u - u_0)] \qquad (u < u_0) \tag{34}$$

This functional form is very accurate for a system which is not too small (i.e., $R_0/\bar{\alpha} > 6$). By inserting Eq. (34) into (12) we have a relation between b and β, so that one of these parameter can be eliminated. The remaining parameter then uniquely determines the initial values $\tilde{\rho}(u)$ and $\tilde{\rho}'(u)$. By varying this parameter we have searched for the solution which satisfies the overall charge neutrality condition. We have checked the internal consistency or the numerical accuracy by confirming that the solution $\tilde{\rho}(u)$ obtained in this way actually satisfies the required boundary condition $\tilde{\rho}'(u_1) = 0$, which is equivalent to the charge neutrality condition (see Appendix A).

Figure 1 shows the calculated ion density profiles at $\bar{\Gamma} = 1$ and $R_1/R_0 = 4$ as well as the MC result. The theoretical $\tilde{\rho}(r)$ for $R_0/\bar{\alpha} = 6.903$ (full curve) is in good agreement with the corresponding MC result[7] in the surface region, although theoretical $\tilde{\rho}(r)$ approaches to the bulk value more slowly than the MC result. The influence of the finite size on $\tilde{\rho}(r)$ is

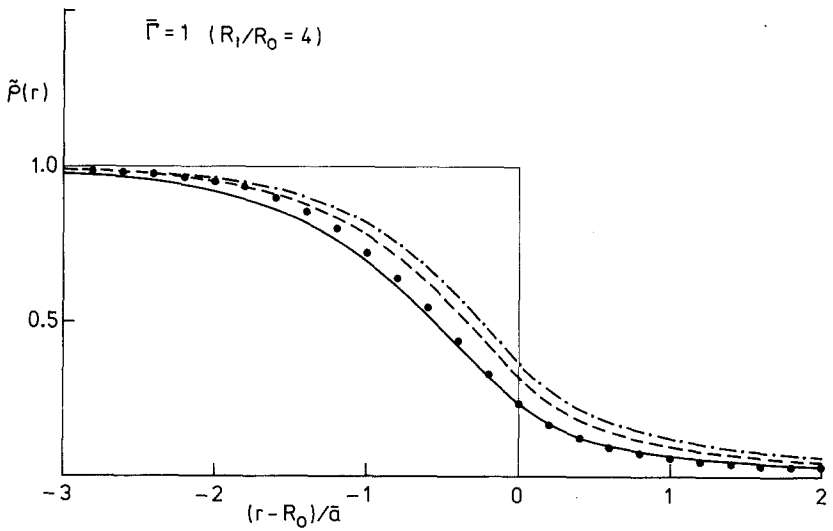

Fig. 1. The size dependence of the surface density profile for a spherical system at $\bar{\Gamma} = 1$ and $R_1/R_0 = 4$. Filled circles are the MC simulation data for $R_0/\bar{\alpha} = 6.903$.[7] Curves are the present results in the PB approximation: Full curve, $R_0/\bar{\alpha} = 6.903$; dashed curve, $R_0/\bar{\alpha} = 20$; chain curve, $R_0/\bar{\alpha} = \infty$ (planar surface).

appreciable even for a very large system. In fact, the spherical system of $R_0/\bar{\alpha} = 20$, which contains about 8000 ions, is still not large enough to produce the density profile for the planar surface.

Figure 2 shows the size dependence of the calculated surface energy U_s for $\bar{\Gamma} = 1$ along with the MC results.[7] To see the influence of a hard wall introduced for ensuring an appropriate equilibrium ion configuration, the results for three different values of R_1/R_0 are shown in this figure. Note that the planar surface in the absence of a hard wall corresponds to the limit $R_0 \to \infty$ with R_1/R_0 fixed at a finite value. All these results in the PB approximation (full curves in Fig. 2) extrapolate quite well to the limiting value $U_s/\bar{\alpha}\bar{\rho}k_B T = 1.08312/(3\bar{\Gamma})^{1/2}$ for the planar surface: We have actually calculated U_s up to $R_0/\bar{\alpha} = 100$. The present result for $R_1/R_0 = 4$ (curve a in

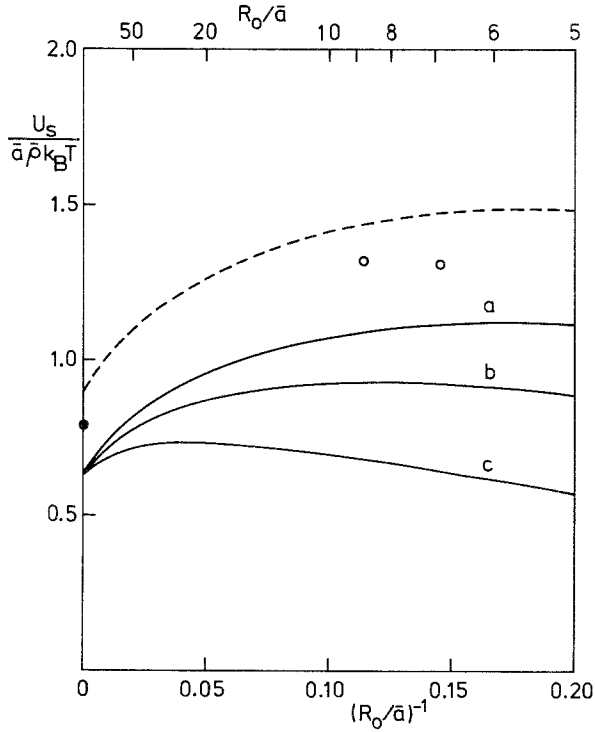

Fig. 2. The size dependence of the surface energy for a spherical system at $\bar{\Gamma} = 1$. Full curves are the present results in the PB approximation: Curve a, $R_1/R_0 = 4$; curve b, $R_1/R_0 = 3$; curve c, $R_1/R_0 = 2$. Dashed curve is the result for $R_1/R_0 = 4$ in the improved PB approximation [including the correction term given by Eq. (37)]. Open circles are the MC results for $R_1/R_0 = 4$.[7] Filled circle is the result of a variational calculation for the planar surface in the square-gradient approximation.[16]

Fig. 2) is nearly saturated for $R_0/\bar{\alpha} < 10$ and in qualitative agreement with the corresponding MC results, although theoretical values are about 20% smaller than the MC results.

The PB approximation is probably not a very good approximation for the purpose of calculating the surface energy even for $\bar{\Gamma} = 1$. In the weak-coupling regime this approximation scheme may be much improved by using the correct free energy density $g_0(\rho)$ in Eq. (4). Alastuey[18] has used this improved PB approximation for calculating the surface density profile of the two-dimensional OCP. In the improved PB approximation we have an extra contribution to the surface free energy given by

$$\Delta\gamma = \frac{1}{4\pi R_0^2} \int d\mathbf{r} [\, g_0^{\mathrm{ex}}(\rho(r)) - g_0^{\mathrm{ex}}(\bar{\rho})\, \theta(R_0 - r)] \tag{35}$$

where $g_0^{\mathrm{ex}}(\rho)$ is the excess free energy density of a uniform OCP of density ρ. In the weak-coupling regime ($\Gamma < 1$) we have fitted $g_0^{\mathrm{ex}}(\rho)$ to the form[16]

$$g_0^{\mathrm{ex}}(\rho) = \rho k_B T(\alpha_1 \Gamma + \alpha_2 \Gamma^{5/4} + \alpha_3 \Gamma^{3/2}) \tag{36}$$

where $\alpha_1 = 0.39327$, $\alpha_2 = -1.11375$, and $\alpha_3 = 0.28419$. The corresponding contribution to the surface energy is then given by

$$\begin{aligned} \Delta U_s &= \Delta\gamma - T\frac{\partial \Delta\gamma}{\partial T} \\ &= \bar{\alpha}\bar{\rho} k_B T \frac{1}{(3\bar{\Gamma})^{1/2}} \frac{1}{u_0^2} \int_0^\infty du\, u^2 \tilde{\rho}(u) \left\{ \alpha_1 \bar{\Gamma} [\tilde{\rho}(u)^{1/3} - 1] \right. \\ &\quad \left. + \frac{5}{4}\alpha_2 \bar{\Gamma}^{5/4} [\tilde{\rho}(u)^{5/12} - 1] + \frac{3}{2}\alpha_3 \bar{\Gamma}^{3/2} [\tilde{\rho}(u)^{1/2} - 1] \right\} \end{aligned} \tag{37}$$

where we have used the charge neutrality condition and $\Gamma(u) = \bar{\Gamma}\tilde{\rho}(u)^{1/3}$.

Noting that the PB approximation reproduces the density profile rather satisfactory (Fig. 1), we have estimated ΔU_s by using the density profiles obtained in that approximation. The agreement between the calculated and MC results is improved by taking into account this contribution (dashed curve in Fig. 2). The discrepancy still remaining between the improved PB and MC results is probably due to the present perturbation approach. As we have noted in the above, the ion density obtained in the PB approximation approaches to the bulk value more slowly than the MC result (Fig. 1). Such a density profile leads to an overestimation of the surface energy. For comparisons, we have also shown in Fig. 2 the result of the variational calculation for the planar surface,[16] which falls between the PB and improved PB results.

Next we proceed to the results of calculations for a slab. For small R_0 ($R_0/\bar{\alpha} < 5$) Eq. (28) can be solved numerically by starting from the initial values of $\tilde{\rho}(u)$ and $\tilde{\rho}'(u)$ at $u = 0$: $\tilde{\rho}'(0)$ is set equal to zero as is required and $\tilde{\rho}(0)$ is treated as the parameter. By varying $\tilde{\rho}(0)$ we have searched for the solution which satisfies the overall charge neutrality condition. For large R_0 ($R_0/\bar{\alpha} > 5$) it is difficult to solve Eq. (28) by the above method. For such cases we have used the asymptotic form given by Eq. (34) to determine the initial values well inside from the surface. We have confirmed that the solutions obtained in these ways satisfy the condition $\tilde{\rho}'(u_1) = 0$ and show the tendency given by Eq. (33).

In the absence of a hard wall ($L_1/L_0 = \infty$) even the ion density profile for a very thin slab with $L_0/\bar{\alpha} = 3$ is hardly distinguishable from that for the limiting planar surface ($L_0/\bar{\alpha} = \infty$). In the presence of a hard wall $\tilde{\rho}(u)$ is raised in the entire region as the consequence of the charge neutrality con-

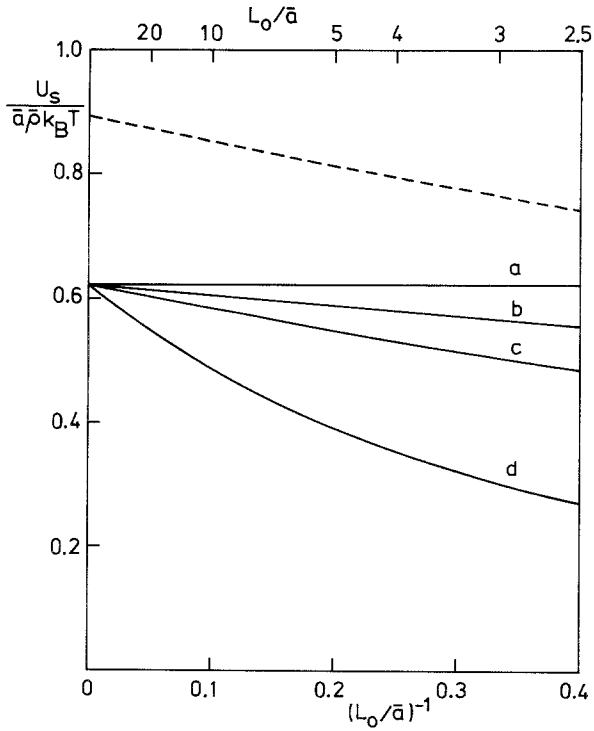

Fig. 3. The thickness dependence of the surface energy for a slab at $\bar{\Gamma} = 1$. Full curves are the present results in the PB approximation: Curve a, $L_1/L_0 = \infty$ (no hard wall); curve b, $L_1/L_0 = 10$; curve c, $L_1/L_0 = 5$; curve d, $L_1/L_0 = 2$. Dashed curve is the result for $L_1/L_0 = 5$ (corresponding to the curve c) in the improved PB approximation.

dition, but its amount is not appreciable if the hard wall is sufficiently distant from the surface of the charge background.

The results of calculations for the surface energy U_s are summarized in Fig. 3. In the absence of a hard wall ($L_1/L_0 = \infty$) calculated values of U_s show virtually no size dependence. The surface energy is lowered if the hard wall is introduced, but its influence on U_s can be reduced to a negligible order by placing it at a sufficiently distant position from the surface (typically, $L_1/L_0 > 10$). The result of the perturbation calculation in the improved PB approximation is also shown in Fig. 3 (dashed curve). These results for a slab might be characteristic, to some degree, to the approximation schemes employed in our calculations, but the qualitative features predicted by these calculations are expected to be real ones in the weak-coupling regime. As far as we are aware, no numerical simulation for a slab has appeared in the literature which can be compared with the present calculations.

4. CONCLUSIONS

The recent MC simulations for the OCP surface[7,8] have raised a serious question about the usefulness of the currently used density functional theory, one of useful means of studying inhomogeneous systems.[15] However, as we have already pointed out,[16] the influence of the finite size on the surface properties could be substantial in a finite system and it would be essential to take into account such an effect when one compares theories for the planar surface with the MC results for a finite system. In this paper we have investigated this problem more rigorously by performing exact calculations for the surface properties of finite systems within the PB approximation scheme. We have also performed perturbation calculations within the improved PB approximation to estimate the contribution to the surface energy which is omitted in the PB approximation.

We have shown that the calculated surface properties for a spherical system ($R_0/\bar{\alpha} < 10$) are quite different from those for the planar surface and are qualitatively in good agreement with the MC results (Figs. 1 and 2). We have also found that the surface energy strongly depends on the position of a hard wall, the introduction of which is essential for achieving an appropriate equilibrium ion configuration. The results of these calculations provide a further supoort for our previous argument that the MC results for a spherical system must be interpreted as including substantial size effects. However, it should be noted that the present calculations are valid only in the weak-coupling regime and the situation could be quite different in the strong-coupling regime. In fact, our variational calculations

for $\bar{\Gamma}=10$ have predicted very small size dependence of the surface energy.[16]

For a slab, on the other hand, such a finite-size effect is very small if the hard wall is introduced at a sufficiently distant position from the surface. Contrary to the case of a sphere, there is no need of introducing a hard wall for a slab and it may be placed at an arbitrarily distant place from the surface. Therefore, a numerical simulation for a slab would be preferred to that for a spherical system, at least in the weak-coupling regime, in order to simulate the planar surface of a semi-infinite system. Unfortunately, such a simulation requires much longer computer time than that for a spherical system.

ACKNOWLEDGMENTS

We thank M. L. Rosinberg for sending us the numerical data of their Monte Carlo simulations. This work is supported by the Grant-in-Aid for Scientific Research No. 57540190.

APPENDIX A: DERIVATION OF EQUATION (17)

Equation (17) can be derived by using a technique of Rosinberg *et al.*[15] generalized to a spherical system. We start from Eq. (12), which may be written

$$\frac{d}{du}\left[\frac{\tilde{\rho}'(u)}{\tilde{\rho}(u)}\right]+\frac{2}{u}\left[\frac{\tilde{\rho}'(u)}{\tilde{\rho}(u)}\right]=\tilde{\rho}(u)-\theta(u_0-u) \tag{A1}$$

We are interested in the ion density which satisfies the physically acceptable boundary condition $\tilde{\rho}'(0)=0$ for a spherically symmetric system. Then, multiplying both sides of Eq. (A1) by $\tilde{\rho}'(u)/\tilde{\rho}(u)$ and integrating, we have

$$\frac{1}{2}\left[\frac{\tilde{\rho}'(u)}{\tilde{\rho}(u)}\right]^2+2\int_0^u \frac{dv}{v}\left[\frac{\tilde{\rho}'(v)}{\tilde{\rho}(v)}\right]^2$$

$$=\begin{cases}\tilde{\rho}(u)-\tilde{\rho}(0)-\ln[\tilde{\rho}(u)/\tilde{\rho}(0)] & (u<u_0)\\ \tilde{\rho}(u)-\tilde{\rho}(0)-\ln[\tilde{\rho}(u_0)/\tilde{\rho}(0)] & (u>u_0)\end{cases} \tag{A2}$$

where we have used $\tilde{\rho}'(0)=0$. From Eq. (A2) we obtain

$$\frac{1}{2}\int_0^{u_1} du\, u^2\left[\frac{\tilde{\rho}'(u)}{\tilde{\rho}(u)}\right]^2+2\int_0^{u_1} du\, u^2\int_0^u \frac{dv}{v}\left[\frac{\tilde{\rho}'(v)}{\tilde{\rho}(v)}\right]^2$$
$$=-\int_0^{u_0} du\, u^2 \ln\tilde{\rho}(u)+\frac{1}{3}u_0^3[1+\ln\tilde{\rho}(u_0)]$$
$$-\frac{1}{3}u_1^3\left\{\tilde{\rho}(0)+\ln\left[\frac{\tilde{\rho}(u_0)}{\tilde{\rho}(0)}\right]\right\} \tag{A3}$$

where we have used the overall charge neutrality condition

$$\int_0^{u_0} du\, u^2[\tilde{\rho}(u)-1]+\int_{u_0}^{u_1} du\, u^2\tilde{\rho}(u)=0 \tag{A4}$$

The second term on the left-hand side of Eq. (A3) can be integrated by part and we have

$$2\int_0^{u_1} du\, u^2\int_0^u \frac{dv}{v}\left[\frac{\tilde{\rho}'(v)}{\tilde{\rho}(v)}\right]^2$$
$$=\frac{2}{3}u_1^3\int_0^{u_1}\frac{du}{u}\left[\frac{\tilde{\rho}'(u)}{\tilde{\rho}(u)}\right]^2-\frac{2}{3}\int_0^{u_1} du\, u^2\left[\frac{\tilde{\rho}'(u)}{\tilde{\rho}(u)}\right]^2 \tag{A5}$$

From (A3) and (A5) we obtain

$$\frac{1}{6}\int_0^{u_1} du\, u^2\left[\frac{\tilde{\rho}'(u)}{\tilde{\rho}(u)}\right]^2$$
$$=\int_0^{u_0} du\, u^2\ln\rho(u)-\frac{1}{3}u_0^3[1+\ln\tilde{\rho}(u_0)]$$
$$+\frac{1}{3}u_1^3\left\{2\int_0^{u_1}\frac{du}{u}\left[\frac{\tilde{\rho}'(u)}{\tilde{\rho}(u)}\right]^2+\tilde{\rho}(0)+\ln\left[\frac{\tilde{\rho}(u_0)}{\tilde{\rho}(0)}\right]\right\} \tag{A6}$$

From (A2) we have relation

$$2\int_0^{u_1}\frac{du}{u}\left[\frac{\tilde{\rho}'(u)}{\tilde{\rho}(u)}\right]^2+\tilde{\rho}(0)+\ln\left[\frac{\tilde{\rho}(u_0)}{\tilde{\rho}(0)}\right]=\tilde{\rho}(u_1) \tag{A7}$$

where we have used $\tilde{\rho}'(u_1)=0$, which can be proved by integrating Eq. (12) from 0 to u_1 and using the charge neutrality condition (A4). Using (A7) in (A6) we finally obtain Eq. (17).

REFERENCES

1. M. Baus and J. P. Hansen, *Phys. Rep.* **59**:1 (1980).
2. P. Choquard, P. Favre, and C. Gruber, *J. Stat. Phys.* **23**:405 (1980).
3. H. Totsuji, *J. Chem. Phys.* **75**:871 (1981).
4. B. Jancovici, *J. Phys. (Paris) Lett.* **42**:L223 (1981); *J. Stat. Phys.* **28**:43 (1982).
5. P. Ballone, G. Senatore, and M. P. Tosi, *Nuovo Cimento* **65B**:293 (1981); *Physica* **119A**:356 (1983).
6. J. P. Badiali and M. L. Rosinberg, *J. Chem. Phys.* **76**:3264 (1982).
7. J. P. Badiali, M. L. Rosinberg, D. Levesque, and J. J. Weis, *J. Phys. C: Solid State Phys.* **16**:2183 (1983).
8. D. Levesque and J. J. Weis, *J. Stat. Phys.* **33**:549 (1983).
9. R. Evans and M. Hasegawa, *J. Phys. C: Solid State Phys.* **14**:5225 (1981).
10. M. Hasegawa and M. Watabe, *J. Non-Cryst. Solids* **61/62**:707 (1984).
11. M. L. Rosinberg, V. Russier, and J. P. Badiali, *J. Non-Cryst. Solids* **61/62**:713 (1984).
12. N. D. Mermin, *Phys. Rev.* **137**:A1441 (1965).
13. R. Evans, *Adv. Phys.* **28**:143 (1979).
14. R. Evans and T. J. Sluckin, *J. Phys. C: Solid State Phys.* **14**:3137 (1981).
15. M. L. Rosinberg, J. P. Badiali, and J. Goodisman, *J. Phys. C: Solid State Phys.* **16**:4487 (1983).
16. M. Hasegawa and M. Watabe, *J. Phys. C: Solid State Phys.* **18**: L573 (1985).
17. P. Ballone, G. Pastore, and M. P. Tosi, *Physica* **128A**:631 (1984).
18. A. Alastuey, *Molec. Phys.* **52**:637 (1984).